

KLiSiF₆ and CsLiSiF₆ – A Structure Investigation

Christiane Stoll,^[a] Markus Seibald,^[b] Dominik Baumann,^[b] Jascha Bandemehr,^[c]
Florian Kraus,^[c] and Hubert Huppertz^{*[a]}

KLiSiF₆ and CsLiSiF₆ were synthesized *via* a high-pressure/high-temperature synthesis route. Even though, both substances crystallize in the orthorhombic crystal system with space group *Pbcn* (no. 60), they show different crystal structures. Main motifs of KLiSiF₆ are an [SiF₆]²⁻ and an [LiF₅]⁵⁻ unit. In contrast, the main motifs of CsLiSiF₆ are an [SiF₆]²⁻ and an [LiF₅]⁴⁻ entity. Within both substances, these units are interconnected and

form 3-dimensional networks. The substances were characterized *via* single-crystal and powder X-ray diffraction, as well as infrared spectroscopy and EDX measurements. Additionally, Mn⁴⁺-doped KLiSiF₆ was analyzed by means of luminescence spectroscopy. It displays line emission in the red spectral region. The maximum emission wavelength is $\lambda_{\text{max}} = 631$ nm.

1. Introduction

Salts of the hexafluorosilicic acid are known since the beginning of the nineteenth century, with K₂SiF₆ first mentioned in 1882.^[1] Recently, many of the ternary alkali metal hexafluorosilicates A₂SiF₆ (A = Li, Na, K, Rb, Cs),^[2–5] as well as the ternary alkaline earth metal hexafluorosilicates A'SiF₆ (A' = Ca, Ba, Sr, Eu)^[6–8] were synthesized and are mentioned in the literature. Additionally, magnesium and strontium hexafluorosilicates are known as hydrates (Mg(SiF₆)(H₂O)₆ and Sr(SiF₆)(H₂O)₂).^[9–10] Nevertheless, a detailed structure description is limited to alkali metal hexafluorosilicates and a few other hexafluorosilicates A'SiF₆ (A' = Ca, Ba, Sr, Eu).^[2–8] All of those described hexafluorosilicates have a common building block, a [SiF₆]²⁻ unit. This unit recently gained lots of attention due to the possibility to partially substitute Si for Mn which results in a narrow line emission in the red spectral region.^[11–13] Anyway, this unit can also be observed within the quaternary hexafluorosilicate KNaSiF₆.^[14] However, it is surprising that just a few quaternary hexafluorosilicates, namely ALiSiF₆ (A = Na, K, Rb, Cs), KNaSiF₆, and Na₃Li(SiF₆)₂ are mentioned in the literature.^[14–15] Currently, the only known crystal structure is the one of KNaSiF₆, which

crystallizes in space group *Pnma* (no. 62).^[14] For the substances KLiSiF₆, NaLiSiF₆, RbLiSiF₆, and CsLiSiF₆, *Skarulis* and *Seibert* predicted the crystal systems as well as the lattice parameters in 1970.^[15] For KLiSiF₆, they determined an orthorhombic unit cell with the lattice parameters *a* = 982.3, *b* = 580.5, and *c* = 756.0 pm. For CsLiSiF₆, a hexagonal unit cell with the lattice parameters *a* = 1133.4 and *c* = 927.1 pm was measured.^[15]

As detailed crystal-structure analyses of both substances, KLiSiF₆ and CsLiSiF₆, are still missing, we took the chance to resolve these structures by means of single-crystal diffraction.

2. Results and Discussion

2.1. Crystal structure of KLiSiF₆

KLiSiF₆ crystallizes in the orthorhombic crystal system with space group *Pbcn* (no. 60) and is isostructural to (NH₄)MnFeF₆ (Pearson code: *oP72* (without H); Wyckoff sequence: *c²d⁸*).^[16] The lattice parameters of KLiSiF₆ are 747.50(3), 1158.58(5), and 979.77(4) pm for *a*, *b*, and *c*, respectively, with a volume of *V* = 0.8485(1) nm³. The single crystal was measured at 203(2) K. It is noticeable that the *b* parameter is twice as large than the one predicted by *Skarulis* and *Seibert* (*a* = 982.3, *b* = 580.5, and *c* = 756.0 pm, *V* = 0.431 nm³).^[15] This is likely a result of an oversight during the indexing of the powder data in 1970. Pictures of the reflections in *0kl*, *1kl*, *h0l*, and *hk0* are depicted in Figure S1. The extinction conditions for the *b*, *c*, and *n* glide reflections can be noticed in *0kl*, *h0l*, and *hk0*, respectively. Upon examination of *1kl*, it becomes evident that there are reflections marking the larger *b*-axis, therefore the unit cell parameters of 747.50(3), 1158.58(5), and 979.77(4) pm for *a*, *b*, and *c*, respectively are found to be correct. The volume of the unit cell amounts to 0.8485(1) nm³. The unit cell contains eight formula units and thus 72 atoms. Within the unit cell, there are two potassium positions, which are located at the special Wyckoff position *4c*, as well as one lithium, one silicon, and six fluorine positions, which are located at the general Wyckoff position *8d*. Further information on the crystal structure refinement can be found in Table 1. Selected distances and angles, as well as atom

[a] Dr. C. Stoll, Prof. Dr. H. Huppertz
Institut für Allgemeine, Anorganische und Theoretische Chemie
Universität Innsbruck
Innrain 80–82, 6020 Innsbruck, Austria
E-mail: hubert.huppertz@uibk.ac.at
<https://www.uibk.ac.at/aatc/mitarbeiter/hub/>

[b] Dr. M. Seibald, Dr. D. Baumann
OSRAM Opto Semiconductors GmbH
Mittelstetter Weg 2, 86830 Schwabmünchen, Germany

[c] J. Bandemehr, Prof. Dr. F. Kraus
Fachbereich Chemie
Philipps-Universität Marburg
Hans-Meerwein-Str. 4, 35032 Marburg, Germany

Supporting information for this article is available on the WWW under <https://doi.org/10.1002/ejic.202000867>

© 2020 The Authors. European Journal of Inorganic Chemistry published by Wiley-VCH GmbH. This is an open access article under the terms of the Creative Commons Attribution Non-Commercial NoDerivs License, which permits use and distribution in any medium, provided the original work is properly cited, the use is non-commercial and no modifications or adaptations are made.

Table 1. Crystal data and structure refinement of KLiSiF ₆ and CsLiSiF ₆ .		
Empirical formula	KLiSiF ₆	CsLiSiF ₆
Molar mass, g mol ⁻¹	188.13	281.94
Crystal system	orthorhombic	orthorhombic
Space group	<i>Pbcn</i> (no. 60)	<i>Pbcn</i> (no. 60)
Powder data		
Powder diffractometer	Stoe Stadi P	Stoe Stadi P
Radiation	Mo-K _{α1} (λ = 70.93 pm)	Mo-K _{α1} (λ = 70.93 pm)
Temperature, K	293(2)	293(2)
<i>a</i> , pm	755.27(2)	926.92(3)
<i>b</i> , pm	1159.61(2)	1146.07(4)
<i>c</i> , pm	982.21(2)	978.33(3)
<i>V</i> , nm ³	0.8602(1)	1.0393(1)
Single-crystal data		
Single-crystal diffractometer	Bruker D8 Quest Photon 100	Bruker D8 Quest Photon 100
Radiation	Mo-K _α (λ = 71.07 pm)	Mo-K _α (λ = 71.07 pm)
<i>a</i> , pm	747.50(3)	922.08(5)
<i>b</i> , pm	1158.58(5)	1142.9(1)
<i>c</i> , pm	979.77(4)	974.01(5)
<i>V</i> , nm ³	0.8485(1)	1.0265(1)
Formula units per cell, <i>Z</i>	8	8
Calculated density, g cm ⁻³	2.945	3.649
Temperature, K	203(2)	173(2)
Absorption coefficient, mm ⁻¹	1.576	7.48
<i>F</i> (000), e	720	1008
2θ range, deg	6.5–75.8	5.7–65.3
Range in <i>hkl</i>	± 12, ± 19, ± 16	± 13, ± 17, ± 14
Total no. of reflections	32109	43802
Independent reflections/ref. parameters/ <i>R</i> _{int}	2289/84/0.035	1877/83/0.043
Reflections with <i>I</i> > 2 σ(<i>I</i>)	1979	1490
Goodness-of fit on <i>F</i> _o ²	1.080	1.055
Absorption correction	semi-empirical (from equivalents)	semi-empirical (from equivalents)
Final <i>R</i> 1/ <i>wR</i> 2 (<i>I</i> ≥ 2σ(<i>I</i>))	0.0188/0.0420	0.0184/0.0406
Final <i>R</i> 1/ <i>wR</i> 2 (all data)	0.0255/0.0438	0.0297/0.0452
Largest diff. peak/hole, e Å ⁻³	0.45/−0.47	1.13/−0.59

coordinates and displacement parameters are reported in the Supporting Information (Tables S1–S4).

The main structural motifs of KLiSiF₆ are two octahedral building blocks represented by an [SiF₆]^{2−} and an [LiF₆]^{5−} unit (Figure 1, top). The Si–F bond lengths within the [SiF₆]^{2−} entity vary from 167.6(1) to 170.1(1) pm (Table S3). This is in accordance with the Si–F bond lengths described for K₂SiF₆ (*d*_{Si–F} = 168.3(2) to 170.6(9) pm).^[3] The F–Si–F angles confirm a distorted octahedral coordination sphere (Table S4). Within the second building unit [LiF₆]^{5−}, the Li–F bond lengths vary from 193.0(1) to 219.4(1) pm (Table S3). This corresponds with the values given in the literature for Li₂SiF₆ (*d*_{Li–F} = 195.5(2) to 216.6(4) pm).^[2] The bond angles are in accordance with a distorted octahedral coordination sphere (Table S4).

These octahedra are connected *via* a common edge and thus form the fundamental building block (Figure 1, bottom). The fundamental building blocks are connected *via* a common corner (F3) and arranged in zigzag lines along [001]. Along [010], the chains are additionally interconnected *via* a common corner (F5). This leads to a formation of six membered rings, which are formed by the centers of six octahedra within the *bc*-plane (Figure 2, right), creating channels along [100] for the potassium cations. Viewed along [010], the interconnection *via* common corners (F6 and F1) between these layers becomes

obvious (Figure 2, right). Every second layer along [100] is shifted, so that [SiF₆]^{2−} and [LiF₆]^{5−} units alternate.

Charge distribution (Chardi)^[17], as well as bond-length/bond-strength calculations (BLBS)^[18–19] confirmed the crystal structure (Table S9). The cation composition of KLiSiF₆ was verified by EDX analysis to be 1:1.0(3) for K:Si. An SEM image is depicted in (Figure S2, left).

2.2. Crystal structure of CsLiSiF₆

CsLiSiF₆ also crystallizes in the orthorhombic crystal system with the space group *Pbcn* (no. 60). The cell parameters are 922.08(5), 1149.2(1), and 974.01(5) pm for *a*, *b*, and *c*, respectively. The volume of the cell amounts to 1.0265(1) nm³. This differs from the unit cell (hexagonal, *a* = 1133.4 and *c* = 927.1 pm, *V* = 1.031 nm³) determined by *Skarulis* and *Seibert*. Transformed into an orthohexagonal projection, the cell parameters amount to *a* = 1133.4, *b* = 1963.05, and *c* = 927.1 pm. Therefore, they can be set into relation with the newly determined cell parameters: *a*_{old} = *b*_{new}, *b*_{old} = *c*_{new} × 2, *c*_{old} = *a*_{new}. As the powder data published by *Skarulis* and *Seibert* (ICDD: 00-023-0895) matches the powder data recorded for the sample prepared during this work (Figure S3), the different

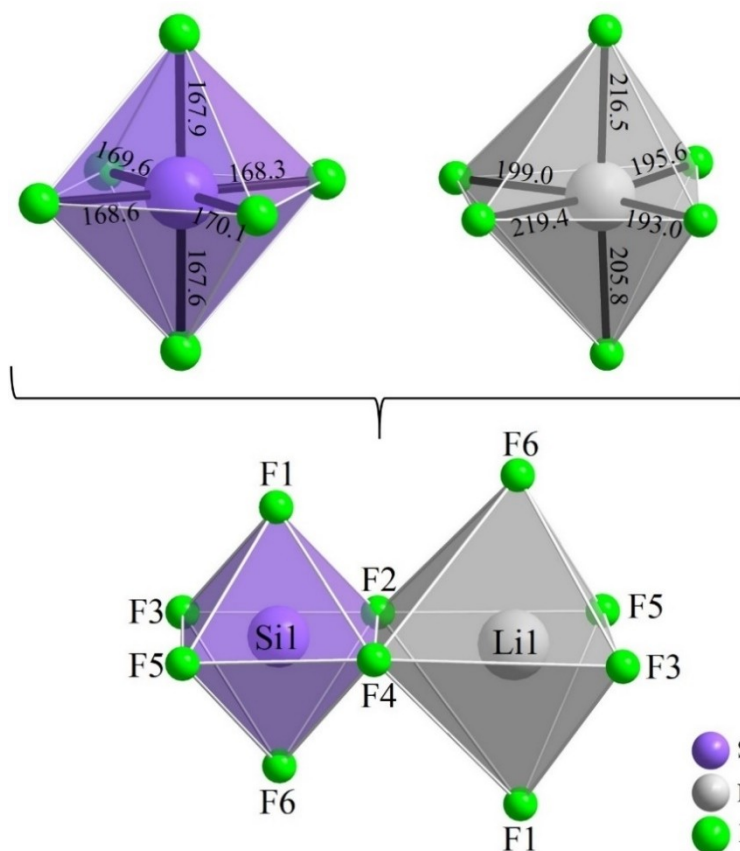


Figure 1. Octahedral coordination sphere of silicon (top-left) and lithium (top-right) in KLiSiF_6 . The connection *via* a common edge is shown in the bottom of the figure.

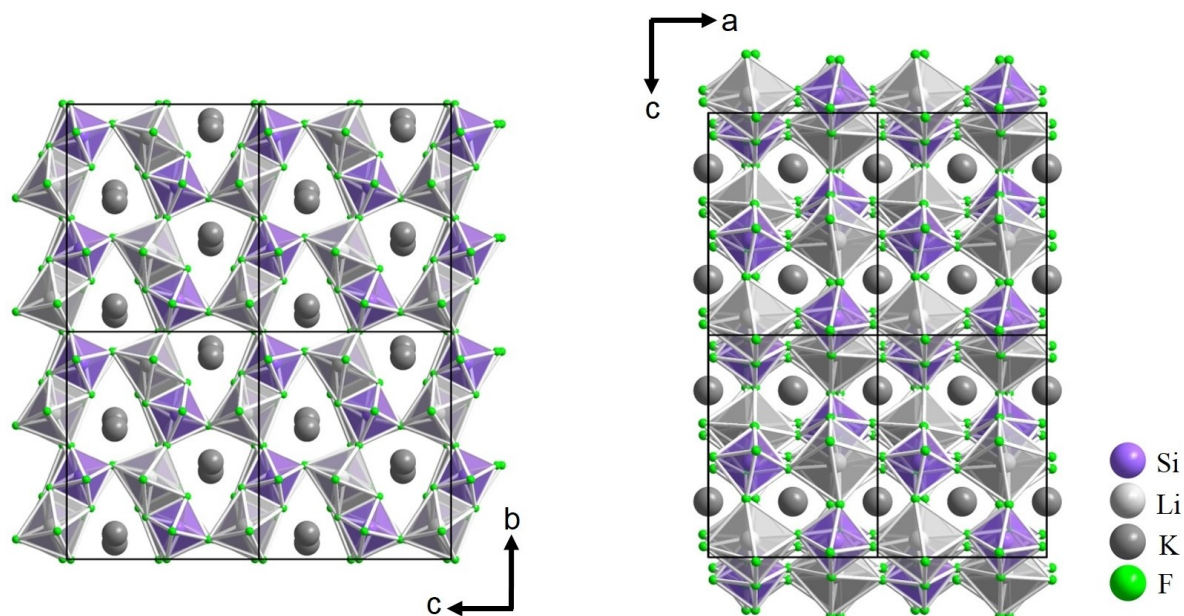


Figure 2. 2×2 unit cells of KLiSiF_6 viewed along $[\bar{1}00]$ (left) and along $[0\bar{1}0]$ (right).

assignment of the crystal system can likely be attributed to a misinterpretation during indexing of the powder data.

The unit cell of CsLiSiF₆ consists of eight formula units including 72 atoms. The asymmetric unit contains two cesium, one lithium, one silicon, and seven fluorine positions. Of these, only the two cesium positions are located at special Wyckoff sites (4c). All other atoms are located at general Wyckoff positions (8d). This leads to a Wyckoff sequence of *c*²*d*⁸ and a

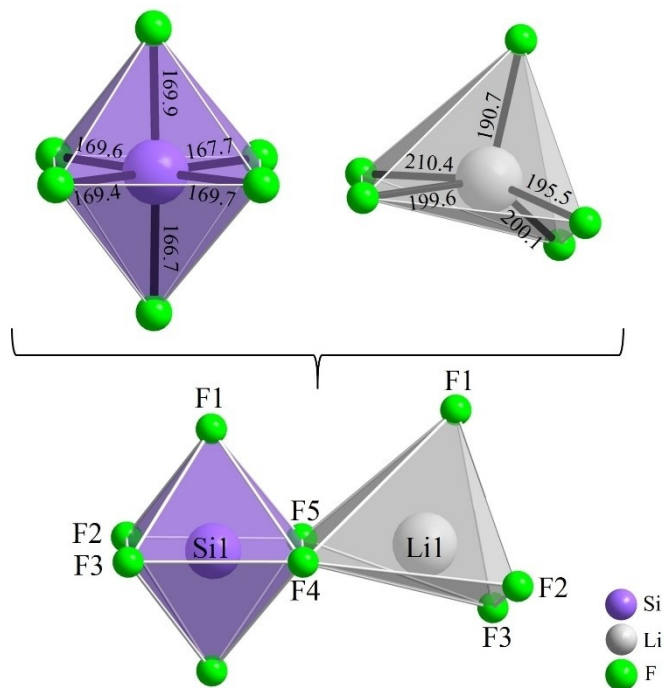


Figure 3. Octahedral coordination sphere of silicon (top-left) and distorted square pyramidal coordination of lithium (top-right) in CsLiSiF₆. The connection *via* a common edge is shown in the bottom of the figure.

Pearson code of *oP72*. Even though, the Wyckoff sequence as well as the Pearson code are equal with the one of KLiSiF₆, CsLiSiF₆ exhibits its own structure type. Information about the crystal structure refinement can be found in Table 1. Furthermore, selected distances, as well as angles, the atom coordinates, and displacement parameters are shown in Tables S5–S8.

Main structural motifs of CsLiSiF₆ are a [SiF₆]²⁻ octahedron (Figure 3, top left) and a [LiF₅]⁴⁻ distorted square pyramid (Figure 3, top right). Within the [SiF₆]²⁻ octahedra, the Si–F bond lengths range from 166.7(2) to 169.9(2) pm (Table S7), which is in accordance with the literature (for K₂SiF₆: *d*_{Si–F} = 168.3(2) to 170.6(9) pm).^[3] The bond angles confirm an octahedral coordination (Table S8). Within the [LiF₅]⁴⁻ unit, the Li–F bond lengths range from 190.7(4) to 210.4(4) pm (Table S7). This unit is also present in Li₂Ta₂O₃F₆ (*d*_{Li–F} = 187(1)–224(2) pm).^[20] The next closest fluorine atom, F1 (*d*_{Li–F} = 335.0 pm), is not part of the coordination sphere according to MAPLE^[21–23] calculations (Table S11). Additionally, the fluorine atom (F6), which would be needed for an octahedral coordination around lithium, is located 401.7(4) pm away from lithium. This is approx. two times the usual bond-length of a Li–F bond. Therefore, a distorted square pyramidal coordination instead of an octahedral one is present within CsLiSiF₆.

These two units are connected *via* a common edge (Figure 3, bottom) building up the fundamental building block of this structure. These building blocks are connected in a similar manner than in KLiSiF₆ and thus build six membered rings within the *bc*-plane (Figure 4, left). Viewed along [010] or [001], the main structural differences between CsLiSiF₆ and KLiSiF₆ become evident. In CsLiSiF₆, lithium is not coordinated octahedrally like in KLiSiF₆ and thus is missing one of the connections to the [SiF₆]²⁻ units. Nevertheless, both units [SiF₆]²⁻ and [LiF₅]⁴⁻ are interconnected in an alternating manner forming a network, if viewed along [010]. Hereby, an [SiF₆]²⁻ unit is connected *via* F1 to the tip of an [LiF₅]⁴⁻ entity. Two of

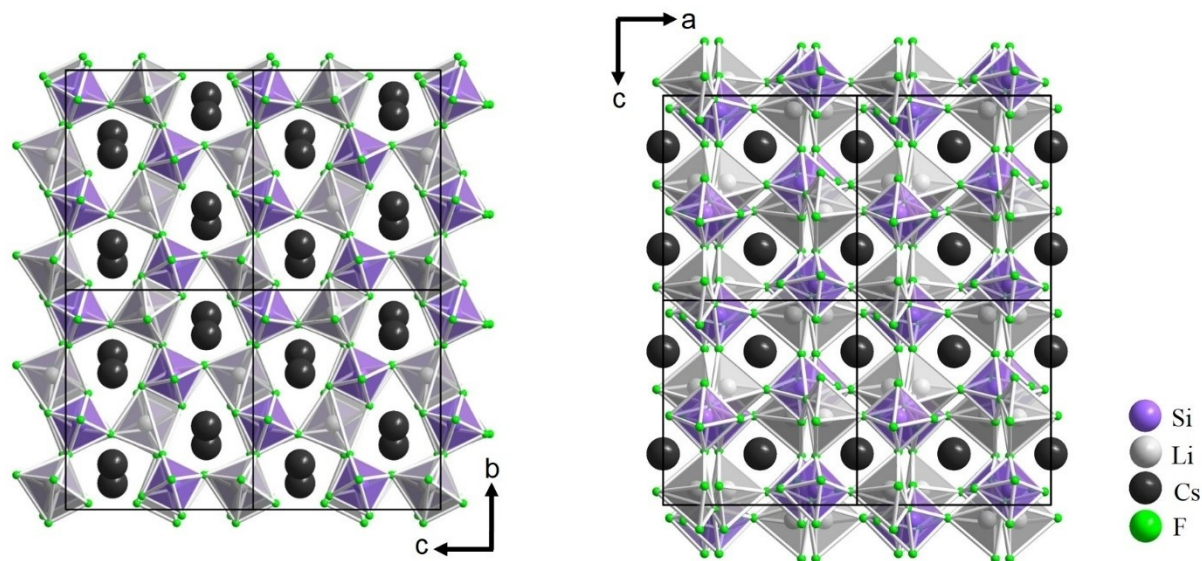


Figure 4. 2 × 2 unit cells of CsLiSiF₆ viewed along [100] (left) and along [010] (right).

these connected units share common corners (F2) and thus form four membered rings within the *ac*-plane. These four membered rings are further interconnected *via* F3 to form a netlike arrangement. Viewed along [00 $\bar{1}$] and in comparison to KLiSiF₆ (Figure 5), an opening of channels for the cesium cations is noticeable. This can likely be attributed to the significantly larger cation radius of Cs⁺ in contrast to the radius of the potassium cation ($r_{\text{Cs}}=202$ pm, CN=12; $r_{\text{K}}=178$ pm, CN=12).^[24] Therefore, to the best of our knowledge, CsLiSiF₆ forms its own structure type.

Chardj^[17] and BLBS^[18-19] calculations confirmed the structural model (Table S10). The cation composition was verified *via* EDX measurements to be 1:1.2(4) for Cs:Si. An SEM image is depicted in Figure S2, right.

2.3. Powder data

Both substances can be synthesized with good yields. Powder analysis *via* the Rietveld technique determined the powder composition of the KLiSiF₆ sample (Figure 6) to be 93.0(1) wt.% KLiSiF₆, with 2.3(1) wt.% Li₂SiF₆ and 4.7(1) wt.% K₂SiF₆ as impurities. The powder sample of CsLiSiF₆ (Figure 7) exhibits CsLiSiF₆ as the main phase with 95.8(2) wt.%, and Li₂SiF₆ and Cs₂SiF₆ as side phases with 0.3(2) wt.% and 4.0(1) wt.%, respectively.

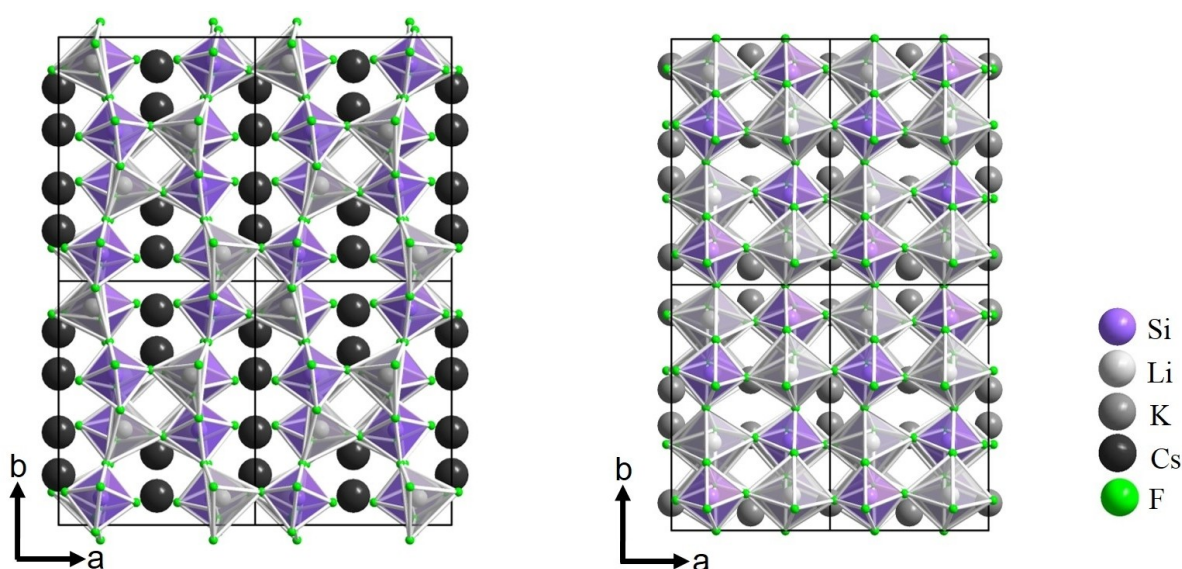


Figure 5. 2×2 unit cells of CsLiSiF₆ (left) and KLiSiF₆ (right) viewed along [00 $\bar{1}$].

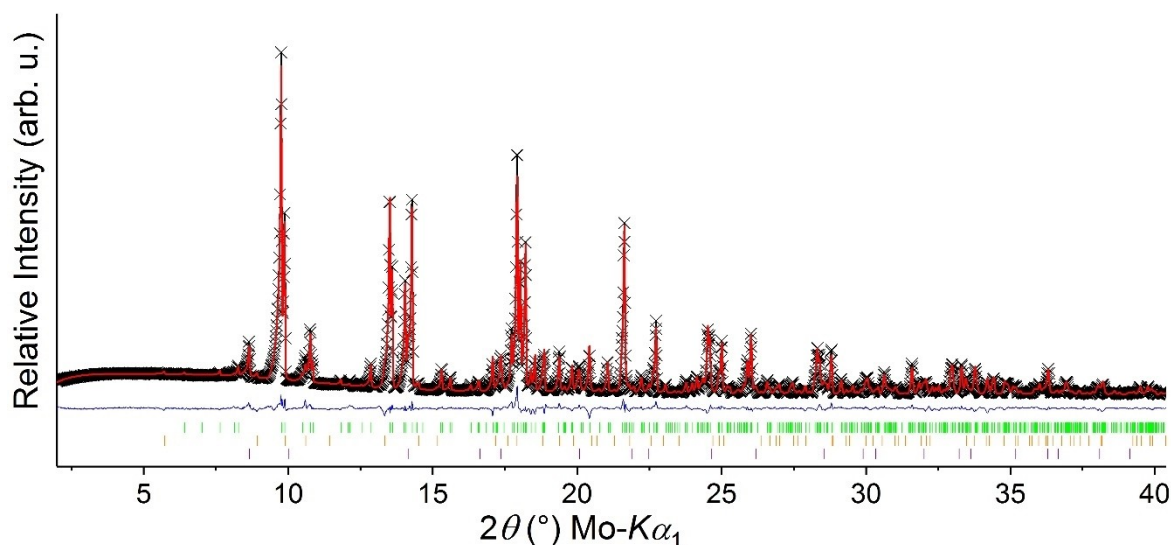


Figure 6. Rietveld plot of the recorded powder pattern (black crosses) of KLiSiF₆. The calculated curve is depicted in red and the difference curve in blue. Bragg positions of KLiSiF₆ are marked in green and the Bragg positions of the side phases Li₂SiF₆ and K₂SiF₆ are marked in orange and purple, respectively.

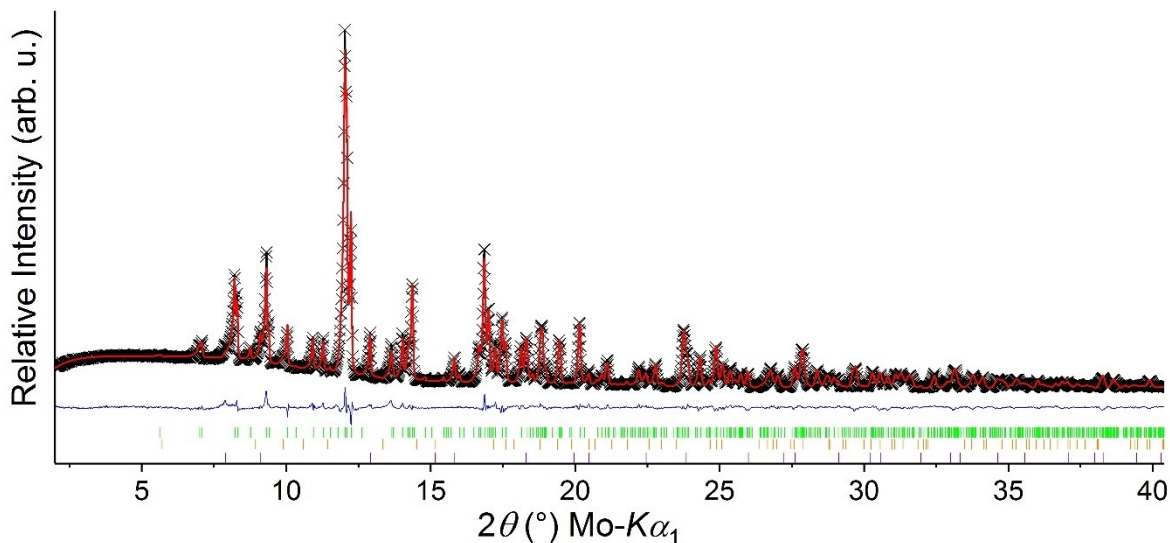


Figure 7. Rietveld plot of the recorded powder pattern (black crosses) of CsLiSiF₆. The calculated curve is depicted in red and the difference curve in blue. Bragg positions of CsLiSiF₆ are marked in green and the Bragg positions of the side phases Li₂SiF₆ and Cs₂SiF₆ are marked in orange and purple, respectively.

2.4. Vibrational spectroscopy

FT-IR spectra of both substances (Figure 8) were measured in the range of 400 to 4000 cm⁻¹. Both show two absorption bands at similar positions (KLiSiF₆: 482 cm⁻¹, 692 cm⁻¹; CsLiSiF₆: 471 cm⁻¹, 702 cm⁻¹). These absorption bands are in accordance

with the ones given for the [SiF₆]²⁻ anion in K₂SiF₆ (first harmonics: ν₄ ≈ 484 cm⁻¹ (deformation), ν₃ ≈ 744 cm⁻¹ (valence)).^[25–27]

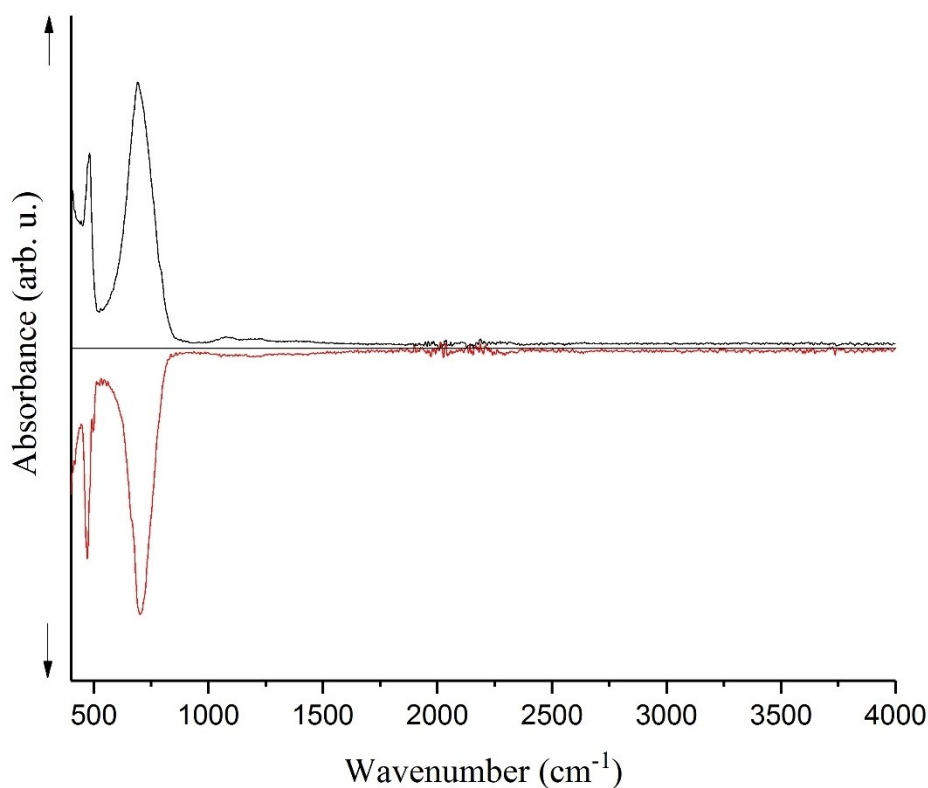


Figure 8. Normalized FT-IR spectra of KLiSiF₆ (black) and CsLiSiF₆ (red) in the range of 400 to 4000 cm⁻¹.

2.5. Luminescence Spectroscopy

Mn⁴⁺ doping of KLiSiF₆ was achieved by a ball-milling experiment. A comparison of the powder pattern before and after the ball-milling step is depicted in Figure S5. There is no difference in the powder pattern, which shows that the majority of crystals did not undergo any structural change during this synthetic step. The product of the ball-milling step, KLiSiF₆:Mn⁴⁺, exhibits red luminescence upon excitation with blue light. The substitution during ball-milling is likely to take place at the surface of the material. Within KLiSiF₆:Mn⁴⁺, Mn⁴⁺ could be substituted onto either, the Si⁴⁺ or the Li⁺ site because of the octahedral coordination. Although we think that the substitution is more likely to take place on the Si⁴⁺ site, because there is no need for charge equalization in the surrounding. An emission spectrum of the polycrystalline sample is shown in Figure 9 (bottom). In comparison to K₂SiF₆:Mn⁴⁺, which does not exhibit a zero-phonon-line, KLiSiF₆:Mn⁴⁺ exhibits a zero-phonon-line (ZPL) and therefore seven emission lines at 598, 609, 613, 622, 631, 635, and 647 nm are noticeable. These belong to the spin and parity forbidden transitions E_g→A_{2g} and correspond to the transitions of the vibronic modes ν₃(t_{1u}), ν₄(t_{1u}), ν₆(t_{2u}), ZPL, ν₆(t_{2u}), ν₄(t_{1u}), and ν₃(t_{1u}), respectively. A ZPL can also be noticed within Li₂SiF₆:Mn⁴⁺, but in comparison the emission line with maximum intensity in KLiSiF₆:Mn⁴⁺ (λ_{max}=631 nm) is slightly red-shifted to the one in Li₂SiF₆:Mn⁴⁺ (λ_{max}=630 nm).^[12] Further measurements of the substance KLiSiF₆:Mn⁴⁺ could not be conducted due to the fact that the non-doped precursor material KLiSiF₆ was synthesized *via* a high-pressure/high-temperature route, which limits the amount of sample available for the doping step.

3. Conclusion

The substances KLiSiF₆ and CsLiSiF₆ were synthesized *via* a high-pressure/high-temperature approach. Although both substances crystallize in the orthorhombic crystal system with space group *Pbcn* (no. 60), they exhibit different crystal structures. KLiSiF₆ is isostructural to (NH₄)MnFeF₆,^[16] whereas CsLiSiF₆ forms its own new structure type. CHARDI and BLBS calculations verify the structural model of both substances, while FT-IR measurements confirm the existence of [SiF₆]²⁻ units within both structures. At first glance, KLiSiF₆ and CsLiSiF₆ might wrongly be described as a solid solution of Li₂SiF₆ and K₂SiF₆ or Cs₂SiF₆ with cation disorder, respectively. Here we present the crystal structure based on single-crystal diffraction data, showing that KLiSiF₆ exhibits a different structure than CsLiSiF₆. Surprisingly, both presented substances do not show the crystal structure of the heavier boundary phase K₂SiF₆ or Cs₂SiF₆, respectively. KLiSiF₆ shows two types of building units, which are connected by common vertices to create a 3D network. CsLiSiF₆ also shows a different structure, revealing a novel structure type, which shows two different fundamental building blocks that are connected to a 3D network. As shown by first experiments, these units are interesting for partial substitution with [MnF₆]²⁻ units, to yield a red luminescent material, as already described for some hexafluorosilicates.^[11–12,28] KLiSiF₆:Mn⁴⁺ exhibits a red luminescence with a maximum emission wavelength of 631 nm. If the materials become easily accessible, the luminescence behavior can be studied in more detail.

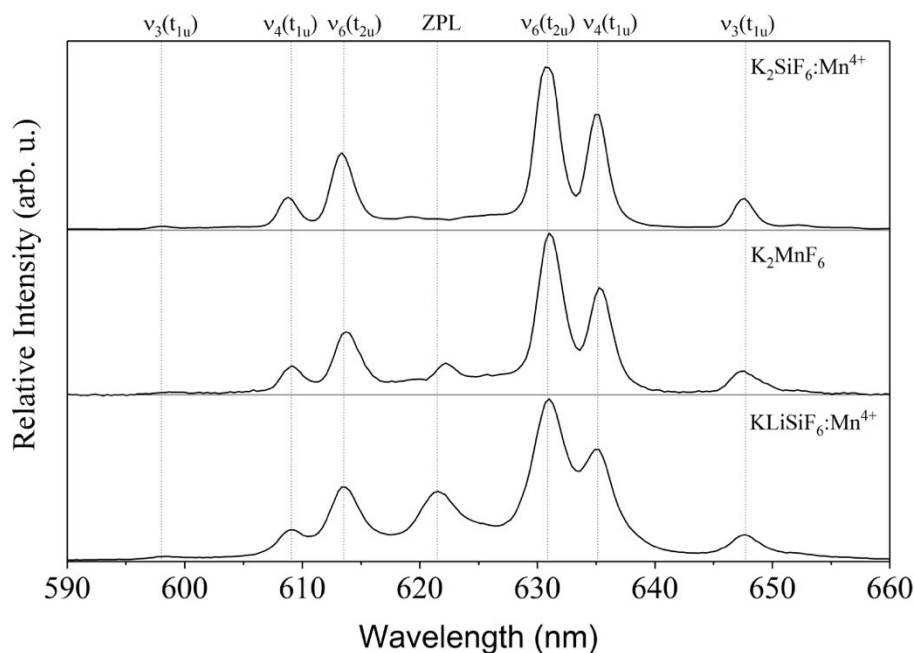


Figure 9. Emission spectrum of KLiSiF₆:Mn⁴⁺ in comparison with the emission spectra of K₂SiF₆:Mn⁴⁺ (state of the art phosphor) and K₂MnF₆ (dopant).

Experimental Section

Synthesis

Single-crystals of KLiSiF_6 and CsLiSiF_6 were synthesized *via* a high-pressure/high-temperature approach. Both syntheses were carried out using a 1000 t multianvil press (Max Voggenreiter GmbH, Mainleus, Germany) equipped with a Walker-type module (Max Voggenreiter GmbH, Mainleus, Germany).

For the synthesis of KLiSiF_6 , the starting materials Li_2SiF_6 and K_2SiF_6 were weighed under argon atmosphere (glove-box, MBraun Inertgas-System GmbH, Germany) with a ratio of 1:1. The starting materials were firmly ground together in an agate mortar and subsequently filled in a platinum capsule (99.95%, Ögussa, Vienna, Austria). This step was followed by the insertion of the capsule into a boron-nitride crucible (Henze Boron Nitride Products AG, Lauben, Germany). The crucible, in turn, was placed into an 18/11 assembly (further details on the assembly are described in literature^[29–31]). The compression of the assembly was achieved by eight tungsten carbide cubes (Hawedia, Marklkofen, Germany), which were placed into the Walker-type module and therefore in the heart of the 1000 t multi-anvil press. Compression of the sample to 5.5 GPa was carried out within 145 min and followed by the heating program, during which the sample was kept at 5.5 GPa. The sample was heated to 750 °C within 10 min and held at that temperature for 150 min, followed by cooling to 350 °C within 180 min. Subsequently, the sample was quenched to RT and the decompression to room pressure was carried out within 430 min. A colourless, crystalline sample was recovered (Figure S4, left).

In a second step, KLiSiF_6 was doped with Mn^{4+} by high-energy ball milling with K_2MnF_6 . For this purpose, 30 mg KLiSiF_6 and 1.7 mg K_2MnF_6 were weighed under argon atmosphere and subsequently transferred into a zirconia vessel together with 200 mg of milling balls ($\varnothing = 1$ mm, ZrO_2). The ball-milling process was carried out in a planetary mill (Pulverisette 7, FRITSCHE, Idar-Oberstein, Germany) at 300 rpm for 6 × 10 min with 15 min breaks in between. A small amount of lightly yellow colored product was recovered.

The synthesis of CsLiSiF_6 was similar. For this synthesis, Li_2SiF_6 and Cs_2SiF_6 were weighed in with a ratio of 1:1 under argon atmosphere. The sample was ground and placed into a platinum capsule, which subsequently was inserted into a boron-nitride crucible. This crucible in turn was placed into a 14/8 assembly (further details on the assembly are described in^[29–31]). Again, the assembly was placed in the middle of eight tungsten carbide cubes, which were inserted into the Walker-type module. The compression of the sample to 5.5 GPa was carried out within 120 min. This step was followed by heating of the sample to 950 °C within 10 min. The temperature was kept for 60 min and subsequently lowered to 400 °C within 120 min. Afterwards the sample was quenched to room temperature and the decompression to room pressure was carried out within 330 min. A colourless, crystalline sample was recovered (Figure S4, right).

X-ray analysis

For the analysis of the powder samples, a Stoe Stadi P powder diffractometer was used. The diffractometer was equipped with a $\text{Ge}(111)$ primary beam monochromator, a Mythen 2 DCS4 detector, and a molybdenum radiation source $\text{Mo-K}_{\alpha 1}$ ($\lambda = 70.93$ pm). The data were recorded within the 2θ range of 2.0–40.4° with a step size of 0.015°.

The samples were covered in perfluoropolyalkylether and single-crystals were mounted on glass fibers under a polarization micro-

scope. For the single-crystal analysis, a Bruker D8 Quest diffractometer (BRUKER, Billerica, USA) was used. An Incoatec microfocus X-ray tube (Incoatec, Geesthacht, Germany) with Mo-K_{α} radiation ($\lambda = 71.07$ pm) and a Photon 100 detector enabled the detection of the intensity data. The data were collected at 203(2) K and 173(2) K for KLiSiF_6 and CsLiSiF_6 , respectively. A multi-scan absorption correction was applied to the intensity data, using SADABS 2014/5.^[32]

Based on the extinction conditions, the space group $Pbcn$ (no. 60) was considered for the structure solution (SHELXTL-XT-2014/4) and found to be correct for the refinement of KLiSiF_6 . Parameter refinement (full-matrix least-squares against F^2) was carried out with SHELXL-2013^[33–34] (implemented in the WinGX-2013.3^[35] suite). The anisotropic refinement led to values of 0.0255 and 0.0438 for $R1$ and $wR2$ (all data), respectively.

For CsLiSiF_6 , the space group $Pbcn$ (no. 60) was considered for the structure solution (SHELXTL-XT-2014/4) based on the extinction conditions. Structure refinement in the same space group was also found to be correct. Parameter refinement (full-matrix least-squares against F^2) was carried out with SHELXL-2013^[33–34] (implemented in the WinGX-2013.3^[35] suite). The anisotropic refinement led to values of 0.0297 and 0.0452 for $R1$ and $wR2$ (all data), respectively.

Deposition Numbers 2031521 (for KLiSiF_6) and 2031520 (for CsLiSiF_6) contain the supplementary crystallographic data for this paper. These data are provided free of charge by the joint Cambridge Crystallographic Data Centre and Fachinformationszentrum Karlsruhe Access Structures service www.ccdc.cam.ac.uk/structures.

EDX-Spectroscopy

Both substances were analysed by energy dispersive X-ray spectroscopy (EDX) using a SUPRATM35 scanning electron microscope (SEM, CARL ZEISS, Oberkochen, Germany, field emission), which was equipped with a Si/Li EDX detector (OXFORD INSTRUMENTS, Abingdon, Great Britain, model 7426).

Vibrational spectroscopy

FT-IR (Fourier Transformed InfraRed) spectra of KLiSiF_6 and CsLiSiF_6 were recorded by a Bruker Alpha-P spectrometer (BRUKER, Billerica, USA). This spectrometer is equipped with a 2 × 2 mm diamond ATR-crystal and a DTGS detector. The software OPUS 7.2 was used for the handling of the data.

Luminescence Spectroscopy

The samples were excited by a blue laser diode with a wavelength of $\lambda = 448$ nm (THORLABS, Newton, USA). The emission spectra were recorded by a CCD-Detector (AVA AvaSpec 2048, AVANTES, Apeldoorn, Netherlands). This single-grain setup was calibrated for spectral radiance prior to the experiments by a tungsten-halogen calibration lamp. Handling of the data was carried out with the software AVA AvaSoft full version 7.

Acknowledgements

We want to express our gratitude to Assoc.-Prof. Dr. Gunter Heymann for the collection of the single-crystal data and to both, Assoc.-Prof. Dr. Gunter Heymann and Dr. Klaus Wurst for the help with the crystal-structure refinement. We also want to thank Christian Koch for the SEM-EDX measurements.

Conflict of Interest

There are no conflicts to declare.

Keywords: Hexafluoridosilicates · Luminescence · Solid-state synthesis · Structure elucidation

- [1] A. Cossa, *J. Chem. Soc. Abstr.* **1988**, 42, 704–706.
 [2] E. Hinteregger, K. Wurst, N. Niederwieser, G. Heymann, H. Huppertz, *Z. Kristallogr.* **2014**, 229, 77–82.
 [3] J. H. Loehlin, *Acta Crystallogr.* **1984**, C40, 570.
 [4] A. Zalkin, J. D. Forrester, D. H. Templeton, *Acta Crystallogr.* **1964**, 17, 1408–1412.
 [5] J. A. A. Ketelaar, *Z. Kristallogr.* **1935**, 92, 155–156.
 [6] S. Frisoni, S. Brenna, N. Masciocchi, *Powder Diffr.* **2011**, 26, 308–312.
 [7] J. L. Hoard, W. B. Vincent, *J. Am. Chem. Soc.* **1940**, 62, 3126–3129.
 [8] R. Latourrette, C. Fouassier, B. Tanguy, P. Hagenmuller, *Z. Anorg. Allg. Chem.* **1977**, 431, 31–38.
 [9] N. I. Golovastikov, N. V. Belov, *Kristallografiya* **1982**, 27, 1084–1086.
 [10] S. Syoyama, K. Osaki, *Acta Crystallogr.* **1972**, B28, 2626–2627.
 [11] S. Adachi, *J. Lumin.* **2018**, 197, 119–130.
 [12] C. Stoll, J. Bandemehr, F. Kraus, M. Seibald, D. Baumann, M. J. Schmidberger, H. Huppertz, *Inorg. Chem.* **2019**, 58, 5518–5523.
 [13] Z. Zhou, N. Zhou, M. Xia, M. Yokoyama, H. T. Hintzen, *J. Mater. Chem. C* **2016**, 4, 9143–9161.
 [14] J. Fischer, V. Krämer, *Mater. Res. Bull.* **1991**, 26, 925–930.
 [15] J. A. Skarulis, J. B. Seibert, *J. Chem. Eng. Data* **1970**, 15, 37–43.
 [16] R. E. Marsh, *J. Solid State Chem.* **1983**, 51, 405–407.
 [17] R. Hoppe, S. Voigt, H. Glaum, J. Kissel, H. P. Müller, K. Bernet, *J. Less-Common Met.* **1989**, 156, 105–122.
 [18] N. E. Brese, M. O’Keeffe, *Acta Crystallogr.* **1991**, B47, 192–197.
 [19] I. D. Brown, D. Altermatt, *Acta Crystallogr.* **1985**, B41, 244–247.
 [20] S. Kaskel, J. Strähle, *Z. Anorg. Allg. Chem.* **1997**, 456–460.
 [21] R. Hoppe, *Angew. Chem. Int. Ed.* **1966**, 5, 95–106; *Angew. Chem.* **1966**, 78, 52–63.
 [22] R. Hoppe, *Angew. Chem. Int. Ed.* **1970**, 9, 25–34; *Angew. Chem.* **1970**, 82, 7–16.
 [23] R. Hübenthal *MAPLE*, v4, University of Gießen, Germany, **1993**.
 [24] R. D. Shannon, *Acta Crystallogr.* **1976**, A32, 751–767.
 [25] R. Stodolski, L. Kolditz, *Z. Chem.* **1985**, 25, 92–93.
 [26] R. D. Peacock, D. W. A. Sharp, *J. Chem. Soc.* **1959**, 2762–2767.
 [27] A. de Lattre, *J. Chem. Phys.* **1952**, 20, 1180–1181.
 [28] T. Takahashi, S. Adachi, *J. Electrochem. Soc.* **2008**, 155, E183–E188.
 [29] H. Huppertz, *Z. Kristallogr.* **2004**, 219, 330–338.
 [30] D. Walker, M. A. Carpenter, C. M. Hitch, *Am. Mineral.* **1990**, 75, 1020–1028.
 [31] D. Walker, *Am. Mineral.* **1991**, 76, 1092–1100.
 [32] G. M. Sheldrick *SADABS v2014/5*, Bruker AXY Inc.: Madison, WI: **2001**.
 [33] G. M. Sheldrick, *Acta Crystallogr.* **2008**, A64, 112–122.
 [34] G. M. Sheldrick, *Acta Crystallogr.* **2015**, C71, 3–8.
 [35] L. J. Farrugia, *J. Appl. Crystallogr.* **2012**, 45, 849–854.

Manuscript received: September 13, 2020
 Revised manuscript received: November 5, 2020
 Accepted manuscript online: November 6, 2020